Eur. Phys. J. C 20, 333–342 (2001)
Digital Object Identifier (DOI) 10.1007/s100520100672

THE EUROPEAN
PHYSICAL JOURNAL C

HQET quark–gluon vertex at one loop

A.I. Davydychev[1,a], A.G. Grozin[2,b]

[1] Department of Physics, University of Mainz, Staudinger Weg 7, 55099 Mainz, Germany
[2] Budker Institute of Nuclear Physics, Novosibirsk 630090, Russia

Received: 8 March 2001 /
Published online: 18 May 2001 –

Abstract. We calculate the HQET quark–gluon vertex at one loop, for arbitrary external momenta, in an arbitrary covariant gauge and space-time dimension. Relevant results and algorithms for the three-point HQET integrals are presented. We also show how one can obtain the HQET limit directly from QCD results for the quark–gluon vertex.

1 Introduction

Heavy quark effective theory (HQET) is an effective field theory meant for approximating QCD for problems with a single heavy quark having mass m when the characteristic momenta of the light fields are much lower than m, and there exists a 4-velocity v such that characteristic residual momenta $k = p - mv$ of the heavy quark are also small. It has substantially improved our understanding of heavy-quark physics during the last decade [1,2]. Methods of perturbative calculations in HQET are reviewed in [3].

In this paper, we calculate the quark–gluon vertex in the leading-order HQET ($1/m^0$) at one loop, for arbitrary external momenta, in an arbitrary covariant gauge, in space-time dimension $d = 4 - 2\varepsilon$. This allows us to take all on-shell limits (introducing additional $1/\varepsilon$ divergences) directly. The general d-dimensional results can also be used for expansion around a dimension other than 4; for example, 2-dimensional HQET was considered in the literature in some detail.

A one-loop calculation of the QCD quark–gluon vertex with a finite quark mass m has recently been completed (see [4], where references to earlier partial results can be found). We check how the HQET result can be obtained by taking the limit $m \to \infty$ in the QCD result.

Let the sum of bare one-particle-irreducible vertex diagrams in HQET (Fig. 1) be $\mathrm{i}g_0 t^a \Gamma^\mu(k, q)$. The "full" momenta of the incoming quark and the outgoing one are

$$p = mv + k, \quad p' = mv + k', \tag{1}$$

where v is the heavy-quark 4-velocity ($v^2 = 1$), and k, k' are the residual momenta. The momentum transfer is

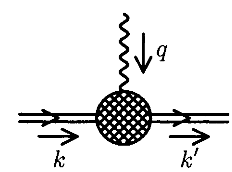

Fig. 1. HQET quark–gluon vertex

$q = p' - p = k' - k$. In the HQET limit, $m \to \infty$, $k \sim k' \sim q \sim \mathcal{O}(1)$. The heavy-quark propagator in HQET is

$$S(k) = \frac{\not{v} + 1}{2} \frac{1}{k \cdot v + \mathrm{i}0}, \tag{2}$$

and the elementary quark–gluon vertex is $\mathrm{i}g_0 t^a v^\mu$.

In the leading-order HQET, heavy-quark propagators and vertices do not depend on the component of the heavy-quark momenta orthogonal to v. Therefore, $\Gamma^\mu(k, q)$ does not depend on $k_\perp = k - (k \cdot v)v$. The only vectors in the problem are v and q, and (see [3])

$$\Gamma^\mu(k, q) = \Gamma_v(\omega, \omega', q^2) v^\mu + \Gamma_q(\omega, \omega', q^2) q^\mu, \tag{3}$$

where

$$\omega \equiv k \cdot v, \quad \omega' \equiv k' \cdot v \tag{4}$$

are the residual energies, and $q \cdot v = \omega' - \omega$. The functions Γ_v and Γ_q can be reconstructed from the contractions

$$\Gamma_v = \frac{(\omega' - \omega)\Gamma^\mu q_\mu - q^2 \Gamma^\mu v_\mu}{Q^2},$$
$$\Gamma_q = \frac{(\omega' - \omega)\Gamma^\mu v_\mu - \Gamma^\mu q_\mu}{Q^2}, \tag{5}$$

where

$$Q^2 \equiv (\omega' - \omega)^2 - q^2 \tag{6}$$

is the 3-momentum transfer squared in the v rest frame.

---

[a] On leave from Institute for Nuclear Physics, Moscow State University, 119899 Moscow, Russia;
e-mail: davyd@thep.physik.uni-mainz.de

[b] e-mail: A.G.Grozin@inp.nsk.su

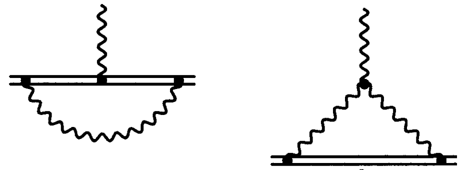

Fig. 2a,b. One-loop vertex diagrams

At the tree level, $\Gamma^\mu = v^\mu$. One-loop corrections are shown in Fig. 2. The contribution Γ_a^μ of the diagram Fig. 2a is proportional to v^μ; that of Fig. 2b has both structures.

The contraction $\Gamma^\mu(k,q)q_\mu$ can be simplified using the identities shown in Fig. 3. Here a gluon line with a black triangle at the end denotes a "longitudinal gluon insertion"; when attached to a vertex, it means just the contraction with the incoming gluon momentum (note that it contains no gluon propagator!). A dot near a propagator means that its momentum is shifted by q. The color structures are singled out as prefactors in front of the propagator differences. The circular arrow in Fig. 3b shows the order of indices in the color structure of the three-gluon vertex $\mathrm{i}f^{abc}$. Two last terms in Fig. 3b contain longitudinal gluon insertions again; for them, the identities of Fig. 3 can be recursively used.

Application of these identities to the diagrams of Fig. 2 is shown in Fig. 4. Here the non-standard vertices of Fig. 5 are $\mathrm{i}g_0 t^a$ and $g_0^2 f^{abc} t^c v^\mu$. This is, of course, just the one-loop case of the general Ward–Slavnov–Taylor identity for the quark–gluon vertex, which is discussed in [5,4] in detail. The one-loop contributions to this identity are collected in (2.28) and (2.29) of [4]. They can easily be associated with the diagrams shown in Fig. 4. The only term which requires some explanation is the diagram involving a one-loop ghost self-energy contribution (the first diagram in the second line of Fig. 4b). It has the form $I_\mu v^\mu$, where the integral I_μ depends on the only vector q; therefore, $I_\mu v^\mu = (q\cdot v)(I_\mu q^\mu)/q^2 = (\omega'-\omega)(I_\mu q^\mu)/q^2$. This can be depicted as in Fig. 6. Thus, this term corresponds to the last contribution on the r.h.s. of (2.29) of [4]. Using Fig. 6, we can avoid introducing the non-standard vertex shown in Fig. 5b.

For the contributions of the diagrams of Figs. 2a,b, we have

$$\Gamma_a^\mu(k,q)q_\mu = \left(1-\frac{C_A}{2C_F}\right)\left(\Sigma(\omega)-\Sigma(\omega')\right), \tag{7}$$
$$\Gamma_b^\mu(k,q)q_\mu = \frac{C_A}{2C_F}\left(\Sigma(\omega)-\Sigma(\omega')\right) + (\text{ghost terms}).$$

Here $-\mathrm{i}\Sigma(\omega)$ is given by the one-loop self-energy diagram of Fig. 7:

$$\Sigma(\omega) = \frac{C_F}{2}\frac{g_0^2}{(4\pi)^{d/2}}\left(2+(d-3)\xi\right)\mathcal{I}(\omega), \tag{8}$$

$$\mathcal{I}(\omega) = -\frac{\mathrm{i}}{\pi^{d/2}}\int\frac{\mathrm{d}^d l}{(l\cdot v+\omega+\mathrm{i}0)(l^2+\mathrm{i}0)} = 2(-2\omega)^{d-3}\Gamma(3-d)\Gamma(d/2-1) \tag{9}$$

(see [9]). In what follows, we shall not explicitly write $+\mathrm{i}0$ in the denominators. Here $\xi = 1-a_0$; a_0 is the bare gauge-fixing parameter. We can see that the Yennie gauge [6] (see also in [7]) is of special interest, since $\Sigma(\omega)$ is finite at $\xi=-2$. Moreover, if the generalization of the Yennie gauge to an arbitrary dimension is chosen as $\xi = -2/(d-3)$ [8], then in the Abelian case (and, in particular, at one loop), the heavy-quark self-energy vanishes [9] (see [3] for a tutorial). The two-loop HQET self-energy was obtained in [9]; the three-loop one can be calculated using the methods of [10]. These calculations are based on integration by parts [11].

Using the identity (7), we can obtain the result for the diagram of Fig. 2a without calculations:

$$\Gamma_a^\mu(k,q) = -\left(1-\frac{C_A}{2C_F}\right)\frac{\Sigma(\omega')-\Sigma(\omega)}{\omega'-\omega}v^\mu. \tag{10}$$

This result is also confirmed by direct calculation. Feynman integrals of the type of Fig. 2a,

$$\int\frac{\mathrm{d}^d l}{(l\cdot v+\omega)^{\nu_1}(l\cdot v+\omega')^{\nu_2}(l^2)^{\nu_3}}, \tag{11}$$

can always be calculated, for integer ν_1, ν_2, by applying

$$\frac{1}{(l\cdot v+\omega)(l\cdot v+\omega')} = \frac{1}{\omega'-\omega}\left[\frac{1}{l\cdot v+\omega}-\frac{1}{l\cdot v+\omega'}\right]$$

the required number of times. We note that in [12] integrals of the type (11) with different velocities v have been examined.

Calculation of Fig. 2b requires more complicated Feynman integrals. A method of their calculation is presented in Sect. 2. Results for the HQET vertex, as well as various limiting cases, are discussed in Sect. 3. Section 4 contains a brief summary of the results obtained. In Appendix A, we present general results for the Feynman integrals of the type of Fig. 2b, for arbitrary d and powers of the denominators. In Appendix B some issues related to the $m\to\infty$ limit of scalar integrals occurring in QCD are examined. In Appendix C, we discuss the relation between the QCD vertex at $k,q \ll m$ and the HQET vertex. In Appendix D, we present the HQET vertex for the heavy-quark scattering in an external gluon field in the background-field formalism.

2 Triangle integrals

2.1 Recurrence relations

We consider the class of Feynman integrals (Fig. 8)

$$V(\nu_0,\nu_1,\nu_2) = -\frac{\mathrm{i}}{\pi^{d/2}}\int\frac{\mathrm{d}^d l}{(l\cdot v+\omega)^{\nu_0}(l^2)^{\nu_1}((l-q)^2)^{\nu_2}}. \tag{12}$$

The cases $\nu_0=0$, $\nu_2=0$, $\nu_1=0$ are trivial; the results are proportional to

$$V(0,1,1) = \mathcal{G}(q^2)$$

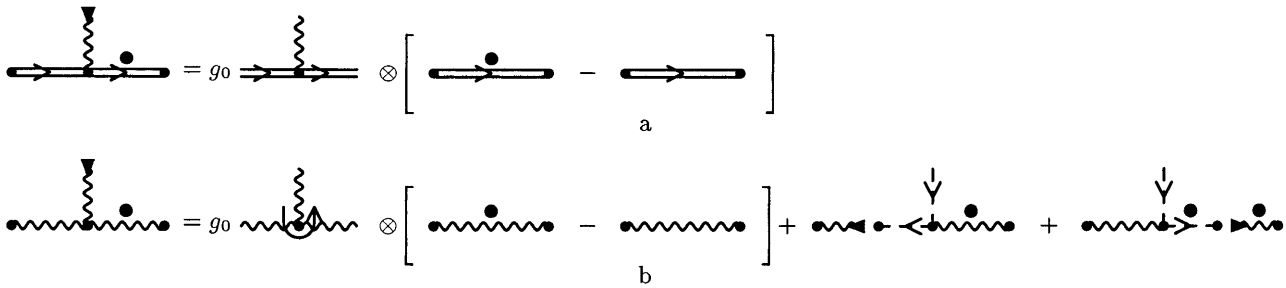

Fig. 3a,b. Longitudinal gluon insertions into quark and gluon propagators

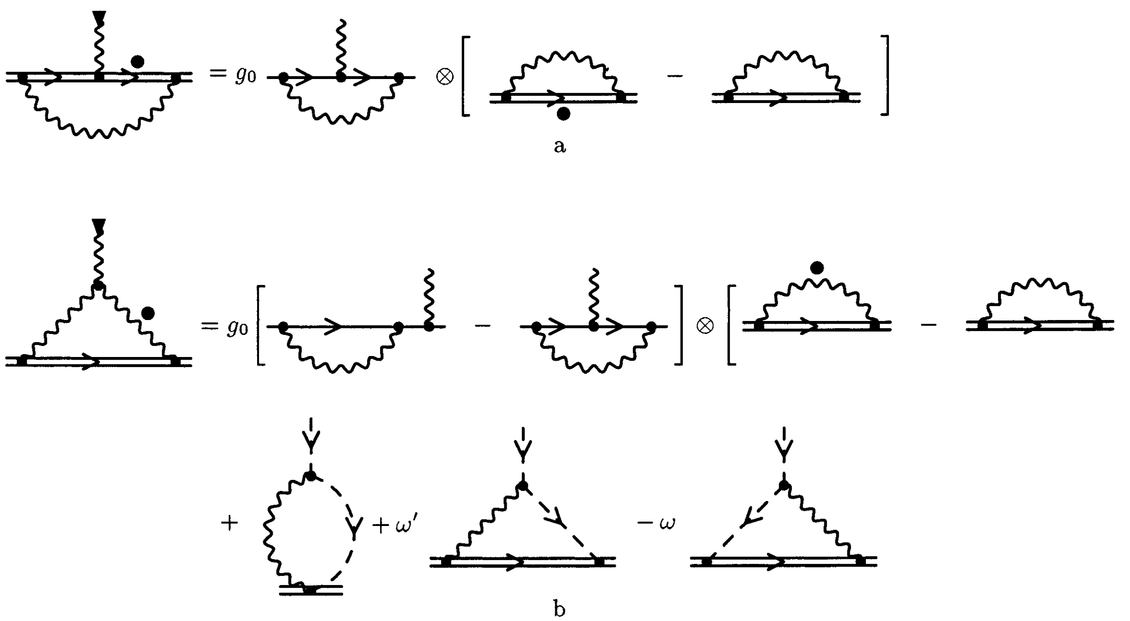

Fig. 4a,b. Ward–Slavnov–Taylor identities for the one-loop vertex

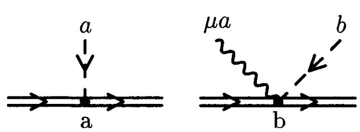

Fig. 5a,b. Non-standard vertices

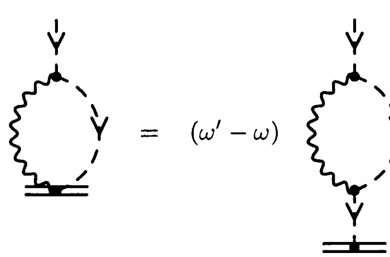

Fig. 6. Relation between ghost self-energy contributions

$$
= (-q^2)^{d/2-2} \frac{\Gamma(2-d/2)\Gamma^2(d/2-1)}{\Gamma(d-2)},
$$

$$
V(1,1,0) = \mathcal{I}(\omega), \quad V(1,0,1) = \mathcal{I}(\omega'). \tag{13}
$$

When all the indices are non-zero, we use integration by parts [11], similarly to [13,9]. Applying the operators

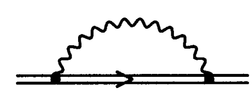

Fig. 7. Heavy-quark self-energy

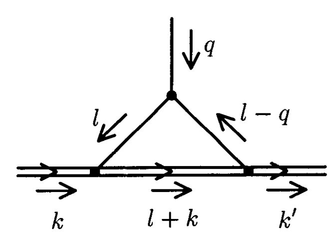

Fig. 8. Feynman integral V

$(\partial/\partial l) \cdot v$, $(\partial/\partial l) \cdot l$, and $(\partial/\partial l) \cdot (l-q)$ to the integrand of (12), we obtain the recurrence relations

$$
\begin{aligned}
&\big[\nu_0 \mathbf{0}^+ + 2\nu_1 \mathbf{1}^+ (\mathbf{0}^- - \omega) \\
&\quad + 2\nu_2 \mathbf{2}^+ (\mathbf{0}^- - \omega')\big] V = 0,
\end{aligned} \tag{14}
$$

$$
\begin{aligned}
&\big[d - \nu_0 - \nu_2 - 2\nu_1 + \omega\nu_0 \mathbf{0}^+ \\
&\quad + \nu_2 \mathbf{2}^+ (q^2 - \mathbf{1}^-)\big] V = 0,
\end{aligned} \tag{15}
$$

$$\left[d-\nu_0-\nu_1-2\nu_2+\omega'\nu_0\mathbf{0}^+ +\nu_1\mathbf{1}^+(q^2-\mathbf{2}^-)\right]V=0, \quad (16)$$

where $\mathbf{0}^\pm V(\nu_0,\nu_1,\nu_2)=V(\nu_0\pm 1,\nu_1,\nu_2)$, etc. When constructing the recurrence procedure we assume that all indices ν_i are integer.

If $\nu_1<0$ and $\nu_2\neq 1$, we can raise ν_1 by (15); if $\nu_1<0$ and $\nu_2=1$, $\nu_0\neq 1$, we can raise ν_1 or ν_2 by (14); if $\nu_1<0$ and $\nu_2=\nu_0=1$, we can raise ν_1 or ν_0 by (16). The case $\nu_2<0$ is symmetric. If $\nu_1>1$, we can lower it or ν_2 by (16); the case $\nu_2>1$ is symmetric. We are left with $V(\nu_0,1,1)$.

Let us take $q^2/2$ times (14), add ω times (16) and ω' times (15), and subtract the $\mathbf{0}^-$ shifted sum of (15) and (16). We obtain at $\nu_1=\nu_2=1$

$$\left[\frac{\Omega}{2}\nu_0\mathbf{0}^+ +(d-2\nu_0-2)(\omega+\omega')-2(d-\nu_0-2)\mathbf{0}^-\right]\times V(\nu_0,1,1) = \left[\mathbf{1}^+\mathbf{2}^-(\omega-\mathbf{0}^-)+\mathbf{2}^+\mathbf{1}^-(\omega'-\mathbf{0}^-)\right]V(\nu_0,1,1), \quad (17)$$

where

$$\Omega\equiv q^2+4\omega\omega'=(\omega'+\omega)^2-Q^2. \quad (18)$$

The integrals on the right-hand side of (17) are trivial. This relation allows us to raise or lower ν_0.

Therefore, all integrals (12) can be expressed, exactly at any d, as linear combinations of three trivial integrals (13) and a non-trivial one, $V(1,1,1)\equiv\mathcal{V}(\omega,\omega',Q)$. An implementation of this algorithm in REDUCE can be obtained at http://wwwthep.physik.uni-mainz.de/Publications/progdata/mzth0101/.

2.2 Master integral

The master integral

$$\mathcal{V}(\omega,\omega',Q)=-\frac{\mathrm{i}}{\pi^{d/2}}\int\frac{\mathrm{d}^d l}{(l\cdot v+\omega)l^2(l-q)^2} \quad (19)$$

is convergent at $d=4$, except for the case $q^2=0$ when it has a collinear divergence (infrared if $q=0$). We shall consider the region $\omega<0$, $\omega'<0$, $q^2<0$, where no real intermediate states exist.

Using the HQET version of the Feynman parameterization (see, e.g., [3])

$$\frac{1}{a^\alpha b^\beta}=\frac{\Gamma(\alpha+\beta)}{\Gamma(\alpha)\Gamma(\beta)}\int_0^\infty\frac{y^{\beta-1}\mathrm{d}y}{(a+by)^{\alpha+\beta}} \quad (20)$$

twice, we have

$$\mathcal{V}=\frac{4\mathrm{i}}{\pi^{d/2}}\int\frac{\mathrm{d}^d l\,\mathrm{d}y\,\mathrm{d}y'}{\left[-yl^2-y'(l-q)^2-2l\cdot v-2\omega\right]^3} = -2\Gamma(1+\varepsilon) \times\int_0^\infty\int_0^\infty\frac{\mathrm{d}y\,\mathrm{d}y'}{(y+y')^{1-2\varepsilon}\left[1-2(\omega y+\omega' y')-q^2yy'\right]^{1+\varepsilon}}, \quad (21)$$

where y and y' have the dimensionality of inverse energy.

For $\varepsilon=0$ ($d=4$), calculating the integral in y' and substituting $y=1/z$, we obtain

$$\mathcal{V}=2\int_0^\infty\frac{\log\dfrac{-q^2-2\omega' z}{z(z-2\omega)}\mathrm{d}z}{(z+Q-\omega+\omega')(z-Q-\omega+\omega')}, \quad (22)$$

where z has the dimensionality of energy. Separating the logarithm as

$$\log\frac{-q^2-2\omega' z}{z(z-2\omega)}=-\log\frac{z-2\omega'}{Q-\omega-\omega'}+\log\frac{-q^2-2\omega' z}{z(Q-\omega-\omega')}$$

and making the substitution $z=(-q^2)/z'$ in the second integral, we obtain the representation

$$\mathcal{V}=-2\int_0^\infty\frac{\log\dfrac{z-2\omega}{Q-\omega-\omega'}\,\mathrm{d}z}{(z+Q-\omega+\omega')(z-Q-\omega+\omega')} -2\int_0^\infty\frac{\log\dfrac{z-2\omega'}{Q-\omega-\omega'}\,\mathrm{d}z}{(z+Q+\omega-\omega')(z-Q+\omega-\omega')}, \quad (23)$$

which is explicitly symmetric under $\omega\leftrightarrow\omega'$. The poles of the denominators at $z=Q\pm(\omega-\omega')$ are compensated by the corresponding zeros of the numerators.

Finally, we obtain

$$Q\mathcal{V}(\omega,\omega',Q)=\mathrm{Li}_2\left(\frac{Q+\omega+\omega'}{2\omega}\right)+\mathrm{Li}_2\left(\frac{Q+\omega+\omega'}{2\omega'}\right) +\mathrm{Li}_2\left(\frac{Q+\omega-\omega'}{2\omega}\right)+\mathrm{Li}_2\left(\frac{Q-\omega+\omega'}{2\omega'}\right) +\log\frac{Q-\omega-\omega'}{-2\omega}\log\frac{Q-\omega+\omega'}{-2\omega} +\log\frac{Q-\omega-\omega'}{-2\omega'}\log\frac{Q+\omega-\omega'}{-2\omega'} -\frac{\pi^2}{3}. \quad (24)$$

This expression has cuts at $\omega>0$, $\omega'>0$, and $Q<|\omega'-\omega|$, where real intermediate states exist.

3 HQET quark–gluon vertex

3.1 General results

Here we present the one-loop HQET vertex, for arbitrary d and ξ. The contribution of the diagram of Fig. 2a was given in (10). For Fig. 2b, we obtain

$$\Gamma_b^\mu q_\mu=\frac{C_A}{2C_F}\left(\Sigma(\omega)-\Sigma(\omega')\right)-C_A\frac{g_0^2}{(4\pi)^{d/2}}\frac{\omega'-\omega}{4\Omega} \times\left\{2(\omega'+\omega)\left[q^2+\omega\omega'(4+(d-4)\xi)\right]\mathcal{V}(\omega,\omega',Q)\right.$$

$$- \left[q^2(4-\xi) + 4\omega\omega'(4+(d-4)\xi)\right] \mathcal{G}(q^2)$$
$$+(d-3)\xi\left(\omega'\mathcal{I}(\omega) + \omega\mathcal{I}(\omega')\right)\}, \quad (25)$$

$$\begin{aligned}
\Gamma_b^\mu v_\mu = C_A \frac{g_0^2}{(4\pi)^{d/2}} \frac{\xi}{8q^2\Omega^2} \{ & -2(d-4)(\omega'+\omega) \\
& \times[(d-6)\xi Q^2 q^2 \omega\omega' \\
& + \Omega Q^2(2q^2 + (4+(d-4)\xi)\omega\omega') \\
& + (2+(d-3)\xi)\Omega q^2 \omega\omega']\mathcal{V}(\omega,\omega',Q) \\
& + [4(d-3)(d-6)\xi q^2 \omega\omega'(\omega'+\omega)^2 \\
& - 2\Omega q^2(q^2 - 4\omega\omega'(d-4+(d-3)\xi)) \\
& + \Omega Q^2((d-4)(4+(d-4)\xi)\Omega \\
& + (d-3)(4-(d-4)\xi)q^2)]\mathcal{G}(q^2) \\
& - (d-3)(d-6)\xi q^2(\omega'+\omega)^2(\omega\mathcal{I}(\omega') + \omega'\mathcal{I}(\omega)) \\
& - (d-3)\Omega[2q^2(\omega'-\omega)(\mathcal{I}(\omega') - \mathcal{I}(\omega)) \\
& + (4+(d-4)\xi)(\omega'^2-\omega^2)(\omega\mathcal{I}(\omega') - \omega'\mathcal{I}(\omega)) \\
& + 2(3+\xi)q^2(\omega\mathcal{I}(\omega') + \omega'\mathcal{I}(\omega))]\}, \quad (26)
\end{aligned}$$

where Ω is defined in (18). We have also derived the first contraction using (7) (Fig. 4). The second contraction vanishes in the Feynman gauge, because the three-gluon vertex yields 0 when contracted with v in all three indices. We also note that there are some cancellations in the generalized Yennie gauge, $\xi = -2/(d-3)$, as well as in the "singular" gauge $\xi = -4/(d-4)$ (which was discussed in [14] in connection with the three-gluon vertex).

If the bare vertex Γ^μ is expressed via the renormalized quantities

$$\frac{g_0^2}{(4\pi)^{d/2}} = \frac{\alpha_s}{4\pi}\mu^{2\varepsilon} e^{\gamma\varepsilon}\left[1+\mathcal{O}(\alpha_s)\right], \quad a_0 = a\left[1+\mathcal{O}(\alpha_s)\right],$$

it should become $Z_\Gamma \Gamma_r^\mu$, where $Z_\Gamma = 1 + Z_1\alpha_s/(4\pi\varepsilon) + \cdots$ is a minimal renormalization constant, and the renormalized vertex Γ_r^μ is finite in the limit $\varepsilon \to 0$. Retaining only the pole parts $\mathcal{I}(\omega) \to 2\omega/\varepsilon$, $\mathcal{G}(q^2) \to 1/\varepsilon$, $\mathcal{V}(\omega,\omega',Q) \to 0$, we obtain, either from (25) or from (26),

$$Z_\Gamma = 1 + \left[(a-3)C_F + \frac{a+3}{4}C_A\right]\frac{\alpha_s}{4\pi\varepsilon}. \quad (27)$$

When $g_0\Gamma^\mu = g\Gamma_r^\mu Z_\alpha^{1/2} Z_\Gamma$ is multiplied by the external leg renormalization factors $Z_Q Z_A^{1/2}$, it should give a finite matrix element. Using

$$Z_A = 1 - \left[\frac{1}{2}\left(a - \frac{13}{3}\right) + \frac{4}{3}T_F n_l\right]\frac{\alpha_s}{4\pi\varepsilon},$$
$$Z_Q = 1 - (a-3)C_F\frac{\alpha_s}{4\pi\varepsilon}$$

(Z_Q follows from (8), n_l is the number of light flavors), we arrive at

$$Z_\alpha = Z_\Gamma^{-2} Z_Q^{-2} Z_A^{-1} = 1 - \beta_0\frac{\alpha_s}{4\pi\varepsilon}, \quad \beta_0 = \frac{11}{3}C_A - \frac{4}{3}T_F n_l. \quad (28)$$

This means that the heavy-quark coupling with the gluon field in HQET is renormalized in the same way as the other QCD couplings. Of course, this must be the case, because otherwise renormalization would destroy gauge invariance of HQET.

3.2 q parallel or orthogonal to v

In the parallel case $q = (\omega'-\omega)v$, $Q = 0$. The denominators of (19) are linearly dependent. Inserting

$$1 = \frac{(l-q)^2 - l^2 + 2(\omega'-\omega)(l\cdot v + \omega)}{\omega'^2 - \omega^2}$$

into the integrand, we obtain

$$\mathcal{V}(\omega,\omega',0) = \frac{1}{\omega'+\omega}\left[2\mathcal{G}\left((\omega'-\omega)^2\right) - \frac{\mathcal{I}(\omega') - \mathcal{I}(\omega)}{\omega'-\omega}\right], \quad (29)$$

exactly at any d.

The vertex Γ^μ is, of course, proportional to v^μ. Therefore, we obtain, either from (25) or from (26),

$$\begin{aligned}
\Gamma_v = 1 & - \left(1 - \frac{C_A}{2C_F}\right)\frac{\Sigma(\omega') - \Sigma(\omega)}{\omega'-\omega} \\
& - C_A\frac{g_0^2}{(4\pi)^{d/2}}\frac{\xi}{4(\omega'+\omega)}\left[(d-3)\frac{\omega'\mathcal{I}(\omega') - \omega\mathcal{I}(\omega)}{\omega'-\omega}\right. \\
& \left. + 2\omega\omega'\frac{\mathcal{I}(\omega') - \mathcal{I}(\omega)}{\omega'^2-\omega^2} + \frac{(\omega'-\omega)^2}{\omega'+\omega}\mathcal{G}((\omega'-\omega)^2)\right]. \quad (30)
\end{aligned}$$

It has an imaginary part, which is contained in $\mathcal{G}((\omega'-\omega)^2)$.

The case when q is orthogonal to v ($\omega' = \omega$, $q^2 = -Q^2$) does not lead to great simplifications. The contribution (10) of Fig. 2a now contains $\mathrm{d}\Sigma(\omega)/\mathrm{d}\omega = (d-3)\Sigma(\omega)/\omega$. The contraction (25) is zero, and hence Γ_b^μ is parallel to v^μ, too. The contribution of Fig. 2b to Γ_v is obtained from (26) by putting $\omega' = \omega$.

3.3 q on the light cone

When $q^2 = 0$, the reduction algorithm of Sect. 2.1 breaks down. All $V(\nu_0,\nu_1,\nu_2)$ with $\nu_0 \le 0$ vanish. We can use (14) to lower ν_0 down to 1. Let us suppose that $\nu_2 > 0$; otherwise, we can interchange $\nu_1 \leftrightarrow \nu_2$, $\omega \leftrightarrow \omega'$. The relation

$$\begin{aligned}
[(d-\nu_0-\nu_1-\nu_2)(\omega'-\omega) - \nu_1\omega' + \nu_2\omega & \\
+ \omega\nu_1\mathbf{1}^+\mathbf{2}^- - \omega'\nu_2\mathbf{2}^+\mathbf{1}^-]V = 0, & \quad (31)
\end{aligned}$$

which is ω' times (15) minus ω times (16), allows us to lower ν_2 down to 1. We are left with $V(1,\nu_1,1)$. Taking (16), subtracting ω' times (14) and adding $2\omega'$ times $\mathbf{1}^+$ shifted (31), we obtain at $\nu_0 = \nu_2 = 1$

$$\begin{aligned}
& \left[d - \nu_1 - 3 + 2\omega'(\omega'-\omega)(d-2\nu_1-4)\mathbf{1}^+\right]V(1,\nu_1,1) \\
& = \left[\nu_1 - 2\omega\omega'(\nu_1+1)\mathbf{1}^+\right]\mathbf{1}^+\mathbf{2}^-V(1,\nu_1,1), \quad (32)
\end{aligned}$$

where the integrals on the right-hand side are trivial. Using this relation, we can lower or raise ν_1 to 0. Therefore, all the integrals $V(\nu_0,\nu_1,\nu_2)$ at $q^2 = 0$ can be reduced to $\mathcal{I}(\omega)$ and $\mathcal{I}(\omega')$. For example, for $V(1,1,1)$ we have

$$\mathcal{V}(\omega,\omega',|\omega'-\omega|) = \frac{(d-3)(\omega'\mathcal{I}(\omega) - \omega\mathcal{I}(\omega'))}{2(d-4)\omega\omega'(\omega'-\omega)}, \quad (33)$$

at arbitrary d.

Repeating, with the new algorithm, the calculation of the diagram in Fig. 2b at $q^2=0$, we obtain

$$\begin{aligned}\Gamma_b^\mu q_\mu &= C_A \frac{g_0^2}{(4\pi)^{d/2}} \frac{1}{8(d-4)\omega\omega'}\\ &\times[2(d-5+(d-3)(d-4)\xi)\omega\omega'(\mathcal{I}(\omega)-\mathcal{I}(\omega'))\\ &-(d-3)(2+(d-4)\xi)(\omega'^2\mathcal{I}(\omega)-\omega^2\mathcal{I}(\omega'))], \quad (34)\end{aligned}$$

$$\begin{aligned}\Gamma_b^\mu v_\mu &= C_A \frac{g_0^2}{(4\pi)^{d/2}} \frac{(d-3)\xi}{16(d-6)\omega^2\omega'^2(\omega'-\omega)}\\ &\times[2(d-6)\omega^2\omega'^2(\mathcal{I}(\omega)-\mathcal{I}(\omega'))\\ &+(2-(d-7)\xi)\omega\omega'(\omega'^2\mathcal{I}(\omega)-\omega^2\mathcal{I}(\omega'))\\ &+(2+(d-5)\xi)(\omega'^4\mathcal{I}(\omega)-\omega^4\mathcal{I}(\omega'))]. \quad (35)\end{aligned}$$

These results can also be obtained from (25) and (26), if we expand the numerator of (26) up to the q^2 term.

The case $q=0$ belongs to all the categories considered above. We obtain, from each of the above results, $\Gamma_q=0$,

$$\begin{aligned}\Gamma_v &= 1-\frac{g_0^2}{(4\pi)^{d/2}}(d-3)\frac{\mathcal{I}(\omega)}{8\omega}\\ &\times\left[4\left(2+(d-3)\xi\right)C_F-\left(4+(d-5)\xi\right)C_A\right], \quad (36)\\ \mathcal{V}(\omega,\omega,0) &= -\frac{(d-3)\mathcal{I}(\omega)}{2\omega^2},\end{aligned}$$

exactly at any d.

3.4 $\Omega=0$

Another interesting case is $\Omega=0$ ($q^2=-4\omega\omega'$). After reducing $V(\nu_0,\nu_1,\nu_2)$ to $V(\nu_0,1,1)$ and trivial integrals (Sect. 2.1), we can use (17) to reduce ν_0 to 0. In particular,

$$\begin{aligned}\mathcal{V}(\omega,\omega',\omega'+\omega) &= \frac{d-3}{2(d-4)(\omega'+\omega)}\\ &\times\left[4\mathcal{G}(-4\omega\omega')-\frac{\mathcal{I}(\omega)}{\omega}-\frac{\mathcal{I}(\omega')}{\omega'}\right], \quad (37)\end{aligned}$$

for any d. Repeating the calculation of the vertex, we obtain

$$\begin{aligned}\Gamma_b^\mu q_\mu &= C_A \frac{g_0^2}{(4\pi)^{d/2}} \frac{1}{16(d-4)(d-6)\omega\omega'(\omega'+\omega)^2}\\ &\times\Big\{4\Big[-(d-6)(4+(d-4)\xi)(\omega'+\omega)^2\\ &+4(d-3)(d-4)\xi\omega\omega'\Big]\omega\omega'(\omega'-\omega)\mathcal{G}(-4\omega\omega')\\ &+\Big[(4(d-6)+(d-3)(3d-16)\xi)(\omega'+\omega)^2\\ &-4(d-3)(d-4)\xi\omega\omega'\Big]\\ &\times(d-4)(\omega'+\omega)(\omega'\mathcal{I}(\omega)-\omega\mathcal{I}(\omega'))\\ &+\Big[(4(d-6)-(d-3)(d-4)(d-8)\xi)(\omega'+\omega)^2\\ &-4(d-3)(d-4)\xi\omega\omega'\Big]\\ &\times(\omega'-\omega)(\omega'\mathcal{I}(\omega)+\omega\mathcal{I}(\omega'))\Big\}, \quad (38)\end{aligned}$$

$$\begin{aligned}\Gamma_b^\mu v_\mu &= C_A \frac{g_0^2}{(4\pi)^{d/2}} \frac{\xi}{32(d-6)(d-8)\omega^2\omega'^2(\omega'+\omega)^2}\\ &\times\Big\{\Big[(d-6)(d-8)(4+(d-4)\xi)(\omega'+\omega)^4\\ &+4(d-8)(2d-(d-3)(d-4)\xi)\omega\omega'(\omega'+\omega)^2\\ &+32(d-3)(d-8-3\xi)\omega^2\omega'^2\Big]\omega\omega'\mathcal{G}(-4\omega\omega')\\ &-\Big[(2(d-7)(d-8)-(d-4)(d-5)\xi)(\omega'+\omega)^2\\ &-4(d-5)(d-8-3\xi)\omega\omega'\Big]\\ &\times(d-3)(\omega'+\omega)(\omega'^2\mathcal{I}(\omega)+\omega^2\mathcal{I}(\omega'))\\ &+\Big[(d-5)(2(d-8)+(d-4)\xi)(\omega'+\omega)^2\\ &+4(d-8-3\xi)\omega\omega'\Big]\\ &\times(d-3)(\omega'-\omega)(\omega'^2\mathcal{I}(\omega)-\omega^2\mathcal{I}(\omega'))\Big\}. \quad (39)\end{aligned}$$

3.5 Quark(s) on the mass shell

If one of the quarks is on its mass shell, say $\omega'=0$, then

$$\begin{aligned}Q\mathcal{V}(\omega,0,Q) &= 2\,\mathrm{Li}_2\left(\frac{Q+\omega}{2\omega}\right)+\log^2\frac{Q-\omega}{-2\omega}\\ &-\frac{1}{2}\log^2\frac{Q-\omega}{Q+\omega}-\frac{2\pi^2}{3} \quad (40)\end{aligned}$$

at $d=4$. The contractions of the vertex are obtained from (25) and (26) by setting $\mathcal{I}(\omega')=0$ and then $\omega'=0$.

When both quarks are on shell ($\omega=\omega'=0$),

$$\begin{aligned}\Gamma_b^\mu q_\mu &= 0, \quad (41)\\ \Gamma_b^\mu v_\mu &= C_A \frac{g_0^2}{(4\pi)^{d/2}} \frac{\xi}{8}\left[-2(4d-13)+(d-4)\xi\right]\mathcal{G}(q^2).\end{aligned}$$

In this case, $\mathcal{V}(0,0,Q)$ does not appear.

It is easy to consider the cases when q is parallel to v and $\omega'=0$, and when $q^2=0$, $\omega'=0$.

4 Conclusion

We have obtained general expressions (10), (25) and (26) for the one-loop HQET quark–gluon vertex. Using the recurrence relations (14)–(17), we expressed the results in terms of one non-trivial integral $\mathcal{V}(\omega,\omega',Q)$ (19) and some trivial integrals (13). For the integral (19) in four dimensions, we have obtained an analytic result (24) in terms of dilogarithms. In Sects. 3.2–3.4 we have also studied some special limits of interest.

In Appendix A we have provided some results for the integrals (12) with arbitrary indices and in arbitrary dimension. We have also discussed, in Appendix B, how the HQET limit can be obtained directly from the standard integrals occurring in the QCD calculation. Using this prescription, in Appendix C we have examined the $m \to \infty$ limit of the general QCD result [4] for the one-loop quark–gluon function, and we have found that it is in agreement with our calculation. We have also presented the result for the background-field vertex (Appendix D).

Acknowledgements. We are grateful to V.A. Smirnov for useful comments on the manuscript, and to T. Mannel and P. Osland for useful discussions. A. G.'s work was supported in part by the RFBR grant 00-02-17646. A. D.'s research was supported by the Deutsche Forschungsgemeinschaft. Partial support from RFBR grant 01-02-16171 is also acknowledged.

Appendix

A One-loop HQET integrals

The result for the two-point HQET integral is well known [9]:

$$I(\nu_0,\nu) \equiv -\frac{\mathrm{i}}{\pi^{d/2}} \int \frac{\mathrm{d}^d l}{(l\cdot v+\omega)^{\nu_0}(l^2)^\nu} = (-1)^{\nu_0+\nu} 2^{\nu_0} (-2\omega)^{d-\nu_0-2\nu} \frac{\Gamma(\nu_0+2\nu-d)\Gamma(d/2-\nu)}{\Gamma(\nu_0)\Gamma(\nu)}. \quad (42)$$

For the triangle integral (12), using Feynman parameters, we arrive at the following double integral representation:

$$V(\nu_0,\nu_1,\nu_2) = \frac{(-1)^{\nu_0+\nu_1+\nu_2} 2^{\nu_0} \Gamma(\nu_0+\nu_1+\nu_2-d/2)}{\Gamma(\nu_0)\Gamma(\nu_1)\Gamma(\nu_2)} \times \int_0^\infty \int_0^\infty \frac{\mathrm{d}y\mathrm{d}y' y^{\nu_1-1} y'^{\nu_2-1} (y+y')^{\nu_0+\nu_1+\nu_2-d}}{[1-2\omega y-2\omega' y'-q^2 y y']^{\nu_0+\nu_1+\nu_2-d/2}}. \quad (43)$$

The symmetry $(\omega,\nu_1) \leftrightarrow (\omega',\nu_2)$ is explicit.

In the special case $\omega=\omega'=0$, the integral (43) can be evaluated in terms of Γ functions,

$$V(\nu_0,\nu_1,\nu_2)|_{\omega=\omega'=0} = (-1)^{\nu_0+\nu_1+\nu_2} 2^{\nu_0-1} \times (-q^2)^{d/2-\nu_0/2-\nu_1-\nu_2} \Gamma(\nu_1+\nu_2+\nu_0/2-d/2) \times \frac{\Gamma(\nu_0/2)\Gamma(d/2-\nu_0/2-\nu_1)\Gamma(d/2-\nu_0/2-\nu_2)}{\Gamma(\nu_0)\Gamma(\nu_1)\Gamma(\nu_2)\Gamma(d-\nu_0-\nu_1-\nu_2)}. \quad (44)$$

In particular, for $\nu_i=1$ we get

$$\mathcal{V}(0,0,Q) = -\frac{\Gamma(1/2)\Gamma((5-d)/2)\Gamma^2((d-3)/2)}{\Gamma(d-3)Q^{1+2\varepsilon}} = -\frac{\pi^2}{Q} + \mathcal{O}(\varepsilon). \quad (45)$$

In another special case, $q^2=0$, we get a hypergeometric function,

$$V(\nu_0,\nu_1,\nu_2)|_{q^2=0} = (-1)^{\nu_0+\nu_1+\nu_2} 2^{\nu_0} (-2\omega)^{d-\nu_0-2\nu_1-2\nu_2} \times \frac{\Gamma(\nu_0+2\nu_1+2\nu_2-d)\Gamma(d/2-\nu_1-\nu_2)}{\Gamma(\nu_0)\Gamma(\nu_1+\nu_2)} \times {}_2F_1\left(\left.\begin{matrix}\nu_2, \nu_0+2\nu_1+2\nu_2-d \\ \nu_1+\nu_2\end{matrix}\right| 1-\frac{\omega'}{\omega}\right). \quad (46)$$

Using simple transformations of the ${}_2F_1$ function, it is easy to see that the result obeys the symmetry $(\omega,\nu_1) \leftrightarrow (\omega',\nu_2)$, as it should. Note that the structure of the result (46) is quite similar to that of the two-point integral with different masses and zero external momentum, see (2.9) of [15]. When $\nu_1=\nu_2=1$, the result (46) reduces to

$$V(\nu_0,1,1)|_{q^2=0} = (-1)^{\nu_0} 2^{d-4} \Gamma(\nu_0-d+3)\Gamma(d/2-2) \times \frac{(-\omega')^{d-\nu_0-3}-(-\omega)^{d-\nu_0-3}}{\omega'-\omega}. \quad (47)$$

Let us represent the denominator of (43) in terms of double Mellin–Barnes integral, expanding with respect to ω and ω' (see, e.g., (3.4) of [15]). Then, the resulting momentum integral can be recognized as

$$V(\nu_0+t_1+t_2, \nu_1+t_1, \nu_2+t_2)|_{\omega=\omega'=0, d\to d+2t_1+2t_2}, \quad (48)$$

where t_1 and t_2 are the contour integration variables. Using (44) we can evaluate the integral (48) in terms of Γ functions. Making a linear substitution for the contour integration variables ($t_1=s+t$, $t_2=s-t$), we arrive at the following double Mellin–Barnes representation for the integral (12):

$$V(\nu_0,\nu_1,\nu_2) = \frac{(-1)^{\nu_0+\nu_1+\nu_2} 2^{\nu_0-1} (-q^2)^{d/2-\nu_0/2-\nu_1-\nu_2}}{\Gamma(\nu_0)\Gamma(\nu_1)\Gamma(\nu_2)\Gamma(d-\nu_0-\nu_1-\nu_2)} \times \frac{1}{(2\pi\mathrm{i})^2} \int_{-\mathrm{i}\infty}^{\mathrm{i}\infty} \int_{-\mathrm{i}\infty}^{\mathrm{i}\infty} \mathrm{d}s\mathrm{d}t \left(-\frac{4\omega\omega'}{q^2}\right)^s \left(\frac{\omega}{\omega'}\right)^t \times \Gamma(-s-t)\Gamma(t-s) \times \Gamma(d/2-\nu_0/2-\nu_1-t)\Gamma(d/2-\nu_0/2-\nu_2+t) \times \Gamma(\nu_0/2+\nu_1+\nu_2-d/2+s)\Gamma(\nu_0/2+s). \quad (49)$$

B QCD integrals in the HQET limit

Here we discuss the relation of massive integrals occurring in standard QCD calculations and HQET integrals. First, let us consider the two-point integral with one massive line and one massless line,

$$J(\nu_0,\nu;m,0) = \int \frac{\mathrm{d}^d l}{[(p+l)^2-m^2]^{\nu_0}(l^2)^\nu}. \quad (50)$$

For general values of ν_0, ν and d, such integrals have been examined in [16,17].

When we substitute $p=mv+k$, the massive denominator in (50) becomes

$$\left[2m(l+k)\cdot v+(l+k)^2\right]^{-\nu_0}. \quad (51)$$

For $k \ll m$, several regions of integration in l are essential. When $l \sim k$, we can expand the heavy propagator (51) in both k/m and l/m, and it becomes the HQET propagator. The leading term of this HQET contribution (called "ultrasoft" in [18,19]) yields $1/m^{\nu_0}$ times an HQET integral (42), which is proportional to $(-2\omega)^{d-\nu_0-2\nu}$, by dimensionality. Higher terms form an expansion in k/m.

Let us subtract and add this expansion of the heavy propagator to the exact one. In the difference, the contribution of small $l \sim k$ is suppressed; typically, $l \sim m$. Therefore, we can expand this integrand difference in regular series in k/m, and integrate term by term. Integrals of all terms of the HQET integrand expansion in k/m vanish in dimensional regularization, because they contain no scale. Therefore, this "hard" contribution can be obtained by expanding the exact QCD integrand (51) in k/m, and integrating term by term. It is analytical at $k = 0$, by construction. The leading term is proportional to $m^{d-2\nu_0-2\nu}$, by dimensionality, whereas the higher terms form an expansion in k/m. This separation of $J(\nu_0, \nu; m, 0)$ at $k \ll m$ into two contributions [17] is a particular case of a more general threshold expansion [18]. Note that k plays the role of the threshold parameter, since $p^2 - m^2 \sim mk$.

We can check these qualitative considerations, using an explicit expression for $J(\nu_0, \nu; m, 0)$. It can be presented in terms of the ${}_2F_1$ function of $z = p^2/m^2$ (see (10) of [16]). Note that in the HQET limit z approaches 1,

$$z = \frac{(mv+k)^2}{m^2}, \quad 1 - z = -\frac{2\omega}{m} - \frac{k^2}{m^2},$$

i.e., it is at the border of convergence of the ${}_2F_1$ function. Transforming from the variable z to $1-z$, we obtain (see also (1.12)–(1.15) of [17])

$$\begin{aligned} J(\nu_0, \nu; m, 0) &= \mathrm{i}\pi^{d/2}(-1)^{\nu_0+\nu} m^{d-2\nu_0-2\nu} \\ &\times \left\{ \frac{\Gamma(\nu_0+\nu-d/2)\Gamma(d-\nu_0-2\nu)}{\Gamma(\nu_0)\Gamma(d-\nu_0-\nu)} \right. \\ &\times {}_2F_1\left(\left. \begin{matrix} \nu, \nu_0+\nu-d/2 \\ \nu_0+2\nu-d+1 \end{matrix} \right| 1-z \right) \\ &+ \frac{\Gamma(\nu_0+2\nu-d)\Gamma(d/2-\nu)}{\Gamma(\nu_0)\Gamma(\nu)} (1-z)^{d-\nu_0-2\nu} \\ &\left. \times {}_2F_1\left(\left. \begin{matrix} d/2-\nu, d-\nu_0-\nu \\ d-\nu_0-2\nu+1 \end{matrix} \right| 1-z \right) \right\}. \end{aligned} \tag{52}$$

We see that the first term here is nothing but the "hard" contribution. It has a prefactor $m^{d-2\nu_0-2\nu}$. The prefactor of the second ${}_2F_1$ function is

$$m^{d-2\nu_0-2\nu}(1-z)^{d-\nu_0-2\nu} \Rightarrow m^{-\nu_0}(-2\omega)^{d-\nu_0-2\nu},$$

up to higher powers of $1/m$. This is the HQET ("ultrasoft") contribution; in the leading order, it yields

$$J(\nu_0, \nu; m, 0) \Rightarrow \mathrm{i}\pi^{d/2}(2m)^{-\nu_0} I(\nu_0, \nu),$$

where $I(\nu_0, \nu)$ is defined in (42).

The value of $(2m)^{\nu_0} J(\nu_0, \nu; m, 0)$ at the singular point $1/m = 0$ is (up to a factor $\mathrm{i}\pi^{d/2}$) the HQET integral (42). When setting $1/m = 0$, we discard the "hard" contribution, which is proportional to $m^{d-\nu_0-2\nu}$, because we can always choose d small enough for this contribution to vanish. The naive Taylor expansion in $1/m$ is given by the HQET contribution. Similarly, the value of $J(\nu_0, \nu; m, 0)$ at the singular point $k = 0$ is the QCD on-shell integral. When setting $k = 0$, we discard the HQET contribution, which is proportional to $(-2\omega)^{d-\nu_0-2\nu}$, because we can always choose d large enough for this contribution to vanish. The naive Taylor expansion in k is given by the "hard" contribution. Neither of these naive expansions, taken separately, describes $J(\nu_0, \nu; m, 0)$ at $k \ll m$. It is given by the sum of both contributions, "hard" and HQET ("ultrasoft") ones (see in [18]).

Now, let us consider off-shell three-point integrals with one massive and two massless internal lines. For arbitrary powers of propagators, such vertex integrals has been considered in [16] (see (25)–(29)) and [20], (4.1)–(4.5). Using the Mellin–Barnes representation, (4.2) of [20] (see also (26) of [16]), we see that two (of three) arguments, p_1^2/m^2 and p_2^2/m^2 (we denote $p_1^2 = k_{23}^2$, $p_2^2 = k_{13}^2$, $p_3^2 = k_{12}^2$) are approaching 1 in our limit, which is at the border of convergence of the corresponding function.

Again, as in the two-point case, we need to construct the analytic continuation of this representation in terms of the variables containing $(m^2 - p_1^2)$ and $(m^2 - p_2^2)$. To do this in the Mellin–Barnes representation, we use the contour-integral version of the corresponding formula for ${}_2F_1$, namely, (A7) of [20] (where we put $\nu_3 = \nu_0$). In this way, we arrive at

$$\begin{aligned} &J_1(\nu_1, \nu_2, \nu_0; m) \\ &= \frac{\mathrm{i}\pi^{d/2}(-1)^{\nu_0+\nu_1+\nu_2} m^{d-2\nu_0-2\nu_1-2\nu_2}}{\Gamma(\nu_1)\Gamma(\nu_2)\Gamma(\nu_0)\Gamma(d-\nu_1-\nu_2-\nu_0)} \\ &\times \frac{1}{(2\pi \mathrm{i})^3} \int \int_{-\mathrm{i}\infty}^{\mathrm{i}\infty} \int \mathrm{d}s \mathrm{d}t \mathrm{d}u \left(\frac{m^2-p_1^2}{m^2} \right)^s \left(\frac{m^2-p_2^2}{m^2} \right)^t \\ &\times \left(-\frac{p_3^2}{m^2} \right)^u \Gamma(-s)\Gamma(-t)\Gamma(-u) \\ &\times \Gamma(d-\nu_0-2\nu_1-2\nu_2-s-t-2u) \\ &\times \Gamma(\nu_0+\nu_1+\nu_2-d/2+s+t+u) \\ &\times \Gamma(\nu_1+t+u)\Gamma(\nu_2+s+u). \end{aligned} \tag{53}$$

Now, we need to analyze the contributions of the poles in the right half-plane of the contour variable u, since they correspond to increasing powers of p_3^2/m^2. There are only two series of poles (with $j = 0, 1, 2, \ldots$),

$$\begin{aligned} &\text{(i)} u = j \quad (\text{due to} \Gamma(-u)) \text{ and} \\ &\text{(ii)} u = d/2 - \nu_0/2 - \nu_1 - \nu_2 - s/2 - t/2 + j/2 \\ &\qquad (\text{due to} \Gamma(d-\nu_0-2\nu_1-2\nu_2-s-t-2u)). \end{aligned}$$

The prefactors contain $m^{d-2\nu_0-2\nu_1-2\nu_2}$ (case (i)) and $m^{-\nu_0}$ (case (ii)). The series (i) yields the "hard" contribution. The HQET ("ultrasoft") contribution is given by the series (ii), whose leading term is $j = 0$. These two contributions are related to the singular limits $1/m = 0$ and $k = q = 0$ in a way similar to the two-point case.

Picking up this leading HQET contribution, we arrive at a double Mellin–Barnes representation (in terms of the remaining contour integrals over s and t), where the kinematical variables involved yield (in the limit $m \to \infty$) the HQET variables,

$$\frac{m^2 - p_1^2}{m\sqrt{-p_3^2}} \to \frac{-2\omega'}{\sqrt{-q^2}}, \quad \frac{m^2 - p_2^2}{m\sqrt{-p_3^2}} \to \frac{-2\omega}{\sqrt{-q^2}}.$$

After introducing the new contour variables $(s+t)/2$ and $(s-t)/2$ we see that the resulting Mellin–Barnes representation is equivalent to (49), so that

$$J_1(\nu_1, \nu_2, \nu_0; m) \Rightarrow \mathrm{i}\pi^{d/2}(2m)^{-\nu_0} V(\nu_0, \nu_1, \nu_2).$$

Therefore, the HQET integrals can be formally obtained *directly* from the standard loop integrals, by picking up the formal Taylor series in $1/m$ which has no prefactors containing m to a power depending on d. Such a prescription is similar to some other prescriptions in dimensional regularization. For instance, considering the massless limit of the integral (50) we need to represent the result in terms of the functions of the variable m^2/p^2, and then discard the contribution containing $m^{-2\varepsilon}$ (see (11) of [16]). We have also demonstrated that the HQET contributions are equivalent to the "ultrasoft" ones, in the language of the threshold expansion [18]. In other words, in the cases considered the exact result is given by the sum of two contributions. The first one is given by a formal Taylor expansion of the integrand in the small parameter of the threshold expansion (the "hard" contribution). The second one is nothing but the HQET series in $1/m$.

C QCD vertex at $m \to \infty$

If we substitute the "hard" parts of all scalar integrals into the QCD vertex, then, in the limit $k \to 0$, $q \to 0$, we just get the on-shell vertex at $q = 0$. Corrections to this limit are regular expansion terms in k/m, q/m. Since we do not consider $1/m$ suppressed terms here, these corrections can be omitted.

If we substitute the HQET parts of all scalar integrals (see Appendix B), we should obtain the HQET vertex, which was calculated in Sect. 3. In order to make a strong check of both the results of [4] (where the one-loop quark–gluon vertex was calculated in arbitrary gauge and dimension) and of the present ones, we consider here the HQET limit of the QCD vertex [4].

Using the standard decomposition of the quark–gluon vertex [21] (see also [22,4]), it can be split into longitudinal and transverse parts,

$$\Gamma^\mu = \sum_{i=1}^{4} \lambda_i L_i^\mu + \sum_{i=1}^{8} \tau_i T_i^\mu, \qquad (54)$$

where λ_i and τ_i are scalar functions depending on kinematical variables, whereas L_i^μ and T_i^μ are vectors which also involve Dirac matrices (see Sect. IID of [4] for further details).

We substitute

$$p_1 = -mv - k - q, \quad p_2 = mv + k, \quad p_3 = q.$$

At the leading order in $1/m$, the initial and final quark spinors obey $\not{v} u = u$. Therefore, we can sandwich Γ^μ between the projectors $(\not{v} + 1)/2$, and use

$$\frac{\not{v}+1}{2}\gamma^\mu \frac{\not{v}+1}{2} = \frac{\not{v}+1}{2} v^\mu \frac{\not{v}+1}{2}.$$

With the required accuracy, there are three independent structures:

$$L_1^\mu \Rightarrow v^\mu + \mathcal{O}(1/m),$$
$$T_3^\mu \Rightarrow q^2 v^\mu - (\omega' - \omega) q^\mu + \mathcal{O}(1/m), \quad T_5^\mu \Rightarrow \frac{1}{2}[\gamma^\mu, \not{q}].$$

The others are

$$L_2^\mu \Rightarrow 4m^2 L_1^\mu + \mathcal{O}(m), \quad L_3^\mu \Rightarrow -2m L_1^\mu + \mathcal{O}(1),$$
$$L_4^\mu \Rightarrow \mathcal{O}(1),$$
$$T_1^\mu \Rightarrow m T_3^\mu + \mathcal{O}(1), \quad T_2^\mu \Rightarrow 2m^2 T_3^\mu + \mathcal{O}(m),$$
$$T_4^\mu \Rightarrow \mathcal{O}(m), \quad T_6^\mu \Rightarrow \mathcal{O}(1), \quad T_7^\mu \Rightarrow \mathcal{O}(m),$$
$$T_8^\mu \Rightarrow m T_5^\mu + \mathcal{O}(1).$$

According to Appendix B, the HQET-relevant "ultrasoft" parts of the scalar integrals are

$$\eta\tilde{\kappa} \Rightarrow 0, \quad \eta\kappa_{2,3} \Rightarrow 0, \quad \eta\kappa_{0,3} \Rightarrow \mathcal{G}(q^2),$$
$$\eta\kappa_{1,2} \Rightarrow \frac{\mathcal{I}(\omega)}{2m}, \quad \eta\kappa_{1,1} \Rightarrow \frac{\mathcal{I}(\omega')}{2m},$$
$$\eta\varphi_1 \Rightarrow \frac{\mathcal{V}(\omega, \omega', Q)}{2m}, \quad \eta\varphi_2 \Rightarrow \frac{1}{(2m)^2}\frac{\mathcal{I}(\omega') - \mathcal{I}(\omega)}{\omega' - \omega},$$

where the notations φ_i, $\kappa_{i,l}$ and η are defined in Sect. IIA of [4].

Therefore, at the leading order $(1/m^0)$ the HQET limit of the QCD vertex (54) yields

$$(\lambda_1 + 4m^2\lambda_2 - 2m\lambda_3) L_1^\mu + (m\tau_1 + 2m^2\tau_2 + \tau_3) T_3^\mu$$
$$+ (\tau_5 + m\tau_8) T_5^\mu.$$

Using the results for λ_i and τ_i listed in [4], we have obtained the result that at the order $1/m^0$ the coefficient of the chromomagnetic structure T_5^μ vanishes, whereas those of L_1^μ and T_3^μ reproduce the results (10), (25) and (26), for arbitrary d and ξ.

Thus the QCD vertex at small k, q is equal to its on-shell value at $k = q = 0$ plus the HQET vertex, up to $1/m$ corrections. We can reformulate this statement: the QCD vertex in the on-shell renormalization scheme is equal to the HQET vertex in the on-shell renormalization scheme, up to $1/m$ corrections. In QCD, the on-shell renormalization subtracts from the one-loop correction its value at $k = q = 0$. In HQET, the on-shell renormalized vertex equals the bare one, because its value at $k = q = 0$ vanishes.

D Background-field vertex

The background-field formalism [23] is convenient for considering heavy-quark scattering in an external gluon field. In this method, the vertex (Fig. 1) with the background gluon differs from the ordinary one. The diagram of Fig. 2a still gives (10), because the quark–gluon elementary vertex does not change. The contraction of the three-gluon vertex with a background gluon momentum contains no ghost terms, just the first difference in Fig. 3b. Therefore,

$$\Gamma_b^\mu q_\mu = \frac{C_A}{2C_F}\left(\Sigma(\omega) - \Sigma(\omega')\right).$$

This is also confirmed by a direct calculation. For the other contraction, we obtain

$$\begin{aligned}
\Gamma_b^\mu v_\mu = {} & C_A \frac{g_0^2}{(4\pi)^{d/2}} \frac{1}{8q^2\Omega^2} \\
& \times \Big\{ 2(\omega' + \omega)[2\Omega^2 q^2 - (d-8)\xi\Omega^2 Q^2 - d\xi\Omega Q^2 q^2 \\
& -(16 + (d^2 - 18d + 40)\xi)\xi\Omega Q^2 \omega\omega' \\
& -(d-3)(d-4)\xi^2 \Omega q^2 \omega\omega' - d^2\xi^2 Q^2 q^2 \omega\omega' \\
& -8(5d-12)\xi^2 Q^2 \omega^2 \omega'^2] \mathcal{V}(\omega, \omega', Q) \\
& + \Big[-8\Omega^2 q^2 + (4(2d-7) - (d-4)\xi)\xi\Omega^2 Q^2 \\
& -8(d-3)(2-(d-5)\xi)\xi\Omega Q^2 \omega\omega' \\
& +4(d-3)(d-4)\xi^2 \Omega q^2 \omega\omega' \\
& -16(d-3)(d-6)\xi^2 Q^2 \omega^2 \omega'^2 \Big] \mathcal{G}(q^2) \\
& +2(d-3)\xi \Big[(2+\xi) q^2 (\omega'^3 \mathcal{I}(\omega) + \omega^3 \mathcal{I}(\omega')) \\
& +2(4 + (d-4)\xi)\omega\omega'(\omega'^2 - \omega^2) \\
& \times(\omega'\mathcal{I}(\omega) - \omega\mathcal{I}(\omega')) \\
& -((1+\xi)\Omega + (d-6)\xi\omega\omega') q^2 \\
& \times(\omega'\mathcal{I}(\omega) + \omega\mathcal{I}(\omega')) \\
& -(q^2 + (6 + (d-5)\xi)\omega\omega') q^2 \\
& \times(\omega\mathcal{I}(\omega) + \omega'\mathcal{I}(\omega')) \Big] \Big\}.
\end{aligned}$$

References

1. M. Neubert, Phys. Rep. **245**, 259 (1994)
2. A.V. Manohar, M.B. Wise, Heavy quark physics (Cambridge University Press, Cambridge 2000)
3. A.G. Grozin, Lectures on perturbative HQET 1, hep-ph/0008300
4. A.I. Davydychev, P. Osland, L. Saks, Phys. Rev. D **63**, 014022 (2001)
5. P. Pascual, R. Tarrach, QCD: Renormalization for the Practitioner, Lecture Notes in Physics, Vol. 194 (Springer, Berlin 1984)
6. H.M. Fried, D.R. Yennie, Phys. Rev. (Ser. 2) **112**, 1391 (1958)
7. A.A. Abrikosov, Zh. Eksp. Teor. Fiz. **30**, 96 (1956); L.D. Soloviev, Dokl. Akad. Nauk SSSR **110**, 203 (1956)
8. A.I. Davydychev, Diploma Thesis, MSU, Moscow, 1984; E.E. Boos, A.I. Davydychev, Preprint INP MSU 88-21/42, Moscow, 1988; G.S. Adkins, Phys. Rev. D **39**, 3798 (1989); D **47**, 3647 (1993)
9. D.J. Broadhurst, A.G. Grozin, Phys. Lett. B **267**, 105 (1991)
10. A.G. Grozin, J. High Energy Phys. **03**, 013 (2000)
11. F.V. Tkachov, Phys. Lett. B **100**, 65 (1981); K.G. Chetyrkin, F.V. Tkachov, Nucl. Phys. B **192**, 159 (1981)
12. A.O. Bouzas, Eur. Phys. J. C **12**, 643 (2000)
13. A.I. Davydychev, J. Phys. A **25**, 5587 (1992)
14. A.I. Davydychev, P. Osland, O.V. Tarasov, Phys. Rev. D **54**, 4087 (1996); D **59**, 109901(E) (1999)
15. A.I. Davydychev, J. Math. Phys. **32**, 1052 (1991)
16. E.E. Boos, A.I. Davydychev, Theor. Math. Phys. **89**, 1052 (1991)
17. J. Gegelia, G.Sh. Japaridze, K.Sh. Turashvili, Theor. Math. Phys. **101**, 1313 (1994)
18. M. Beneke, V.A. Smirnov, Nucl. Phys. B **522**, 321 (1998); V.A. Smirnov, hep-ph/0101152
19. V.A. Smirnov, Phys. Lett. B **465**, 226 (1999)
20. A.I. Davydychev, J. Math. Phys. **33**, 358 (1992)
21. J.S. Ball, T.-W. Chiu, Phys. Rev. D **22**, 2542 (1980)
22. A. Kızılersü, M. Reenders, M.R. Pennington, Phys. Rev. D **52**, 1242 (1995)
23. L.F. Abbott, Nucl. Phys. B **185**, 189 (1981); Acta Phys. Pol. B **13**, 33 (1982)